NOTATION

a = interfacial area per volume of transfer device, sq. ft./cu. ft.
A = interfacial transfer area, sq. ft.
C = solute concentration in liquid, lb./cu. ft.; C_i, at the interface; C_s, in equilibrium with bulk gas phase; C_0, at time zero; C_1, upstream from the device and uniform tank concentration; C_2, downstream; (C' refers to parts per million $= C \times 10^6/\rho$)
H = Henry's law constant for the same concentration units in gas and liquid phases, dimensionless
k_L, k_G = liquid and gas film transfer coefficients, ft./min.
K_L = overall liquid transfer coefficient, ft./min.
m = slope of the line resulting from a plot of Equation (7), liter/min.
ΔP = pressure drop across device, in. Hg
r = rate of transfer, lb. mass of solute/min.
V = liquid volume in system, cu. ft.
w = liquid flow rate, lb. mass/min.
θ = time, min.
ρ = liquid density, lb. mass/cu. ft.

LITERATURE CITED

1. Am. Pub. Health Ass'n., Inc., "Standard Methods for the Examination of Water, Sewage, and Industrial Wastes," 10 ed., p. 252, New York (1955).
2. Bauer, W. G., A. G. Fredrickson, and H. M. Tsuchiya, *I/EC Process Design and Dev.*, **2**, 178 (1963).
3. Cooper, C. M., G. A. Fernstrom, and S. A. Miller, *Ind. Eng. Chem.*, **36**, 504 (1944).
4. Cullen, E. J., and J. F. Davidson, *Chem. Eng. Sci.*, **6**, 49 (1956).
5. Dobbins, W. E., C. E. Carver, and E .L. Gaden, "Biological Treatment of Sewage and Industrial Wastes," McCabe and W. W. Eckenfelder, eds., Vol. 1, pp. 141, 149, 172, Reinhold, New York (1956).
6. Drier, D. E., *ibid.*, p. 215.
7. Eckenfelder, W. W., *Chem. Eng. Progr.*, **52**, 286 (1956).
8. Furgason, R. R., and M. L. Jackson, "Proceedings of 15th Industrial Waste Conference," *Engr. Bull.* 106, p. 258, Purdue University, Lafayette, Indiana (1960).
9. Gimpel, H. E., M.S.Ch.E. thesis, University of Idaho, Moscow, Idaho (1961).
10. Hauxwell, G. D., M.S.Ch.E. thesis, University of Idaho, Moscow, Idaho (1959).
11. Ho, C. C., M.S.Ch.E. thesis, University of Idaho, Moscow, Idaho (1960).
12. Jackson, M. L., and W. D. Collins, *Ind. Eng. Chem. Process Design Develop.*, **3**, 386 (1964).
13. Kolthoff, I. M., and J. J. Lingane, "Polarography," p. 244, Interscience, New York (1941).
14. Kountz, R. R., "Biological Treatment of Sewage and Industrial Wastes," J. McCabe, and W. W. Eckenfelder, ed., Vol. 1, p. 212, Reinhold, New York (1956).
15. ———, and J. C. Villforth, "Proc. 9th Ind. Waste Conf.," Eng. Ext. Series No. 87, p. 53, Purdue Univ., Lafayette, Indiana (1954).
16. Rand, M. C., and H. Henkelekian, *Sewage and Industrial Wastes*, **23**, 1141 (1951).
17. Toor, H. L., and J. M. Marchello, *A.I.Ch.E. Journal*, **4**, 97 (1958).
18. Weston, R. F., "Proc. 16th Ind. Waste Conf.," Eng. Ext. Series 109, p. 505, Purdue Univ., Lafayette, Indiana (1961).
19. Yoshida, F., A. Ikeda, S. Imakawa, and Y. Miura, *Ind. Eng. Chem.*, **57**, 435 (1960).

Manuscript received November 25, 1963; revision received April 10, 1964; paper accepted April 13, 1964. Paper presented at A.I.Ch.E. Memphis meeting.

Mass Transfer in a Fluidized Bed Crystallizer

S. H. BRANSOM and G. A. R. TROLLOPE

University of Manchester, Manchester, England

Continuous crystallizers represent a wide range of mass transfer equipment types, from stirred tanks to tubular reactors. Except for stirred tanks however there are no analyses of operating characteristics which can be used for design or scale-up calculations. In other types of crystallizers the variables are inter-related in a complicated manner, and few of the basic design data are available. Even for the case of a stirred tank, where there are fewest variables, the basic kinetic data are scarce. Crystallizing velocities have been measured for many materials (*1*), but few are in the form suitable for plant design and few have been measured under conditions even approximating plant operation.

It was the purpose in the present experiments to examine the characteristics of the so-called *classifying* type of crystallizer. The extent of size classification in a fluidized bed is small however, and it has been shown (*2*) that there is an apparent advantage to be gained by increasing the stirring action in this type of machine. The complex pattern of the supersaturated liquor distribution under such conditions makes it practically impossible to analyze or predict performance. If a fluidized bed crystallizer is designed and operated to approximate to plug flow of the liquor, then an analysis of the mass transfer processes in terms of the diffusional effects and the surface reaction would be simplified. The important secondary processes such as the generation of new nuclei, the effects of suspension density, etc., cannot be correctly interpreted until the most fundamental processes are understood.

It was shown in an earlier paper (*3*) that if a fluidized bed crystallizer is regarded as a tubular reactor with a low dispersion number, that is essentially plug flow, certain characteristics can be calculated from the basic rate equation for crystallizing velocity expressed as

$$dL/dt = k \cdot (N'_{Re})^b \cdot S^n \qquad (1)$$

$(N'_{Re})^b$ takes the effect of eddy diffusivity of the liquor into account in an empirical manner, and when the liquor density and viscosity can be taken as constant, this term can be conveniently abbreviated to L^b. While plug flow of the liquor was assumed for each case, it was shown that the behavior of the suspended crystals affects the characteristics of the process. Tentative solutions were proposed for the cases of complete mixing of the crystals in the bed and for exact size classification. Bennett (*4*) has shown that the size distributions of crystals, taken from industrial machines, differed from those predicted for the simplified models. This is to be expected since the ma-

chines depart considerably from the conditions assumed for the models.

Some preliminary experiments were carried out on a pilot scale crystallizer to test the validity of the model and are reported elsewhere (5). The results confirmed that mass transfer was governed by kinetics described by Equation (1), but a number of complications were encountered, particularly in connection with size classification and with the distribution of the entrant liquor in the lower parts of the bed. The present experiments were designed on the basis of the earlier experience to minimize the errors arising from such complications. For example the entrant liquor was introduced over the whole cross section of the bottom of the bed in order to minimize the effects of radial dispersion of the liquor. Lemlich and Caldas (6) have shown that radial temperature profiles during heat transfer in liquid-fluidized beds are flat over a wide range of velocity except for a narrow region close to the wall. On the other hand Kramers et al. (7) found a 4 to 5-fold variation in longitudinal dispersion over a radial traverse in a similar system. In the present discussion radial dispersion has been neglected as a first approximation.

The decay of the driving force for mass transfer was measured by measuring the solute concentration at various points along the suspended bed. Thus no account had to be taken of backmixing in entry or exit sections as for the cases of reactor models considered by Danckwerts (8), Wehner and Wilhelm (9), and others. While plug flow of the liquor has been assumed, the movement of crystals in the bed may contribute to the dispersion of supersaturation. Any circulation of the crystals will transport concentrated liquor up and spent liquor down the bed, and fluctuations in the suspension density may allow pockets of liquor to bypass regions of momentarily high density. Both effects, which tend to reduce the concentration gradient in the bed, may be accounted for by an effective eddy diffusivity or as a fraction of stream bypassing.

A mass balance across a horizontal element of suspension, of thickness dH, at a distance H from the bottom of the bed and of unit area cross section is given by

$$\delta_E \frac{d^2C}{dH^2} - u\frac{dC}{dH} - kA(C - C^x)^n = 0 \qquad (2)$$

The velocity constant k is defined in terms of mass transferred to unit area of crystal in unit time under unit driving force, that is unit mass of excess solute in unit volume of liquor. C^x is the equilibrium concentration of solute at the temperature in question. Levenspiel and Bischoff (10) have given graphical solutions of Equation (2) for the cases of $n = 1$ and $n = 2$, but the system used was found to conform to first order in $(C - C^x)$; Equation (2) is solved directly to give

$$C(H) - C^x = [C_o - C^x] \exp\left[\left(\frac{u - \sqrt{u^2 + 4A\delta_E k}}{2\,\delta_E}\right)H\right] \qquad (3)$$

where $C_o - C^x$ is the supersaturation S_o at the bottom of the crystal bed, and $C(H) - C^x = S(H)$ is the supersaturation at distance H from the bottom. The experimental values of $S(H)$ at known values of H yield the exponent as H and a factor m given by

$$S(H) = S_o \exp(m \cdot H) \qquad (4)$$

The factor m is a function of the operating variables, and by comparison with Equation (3) the model requires that these variables are summarized by the liquor velocity, the area of crystal in unit volume of suspension, and the eddy diffusivity. Whether the velocity constant k is fixed by the materials and the temperature or also depends on the crystallizer design remains to be discovered.

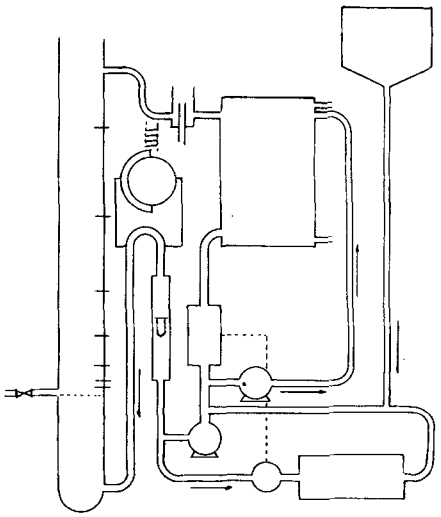

Fig. 1. The pilot-scale continuous crystallizer. (Diagrammatic and not to scale.)

The analytical solution for the fractional bypassing model is less simple, but a practical result may be calculated by dividing the bed into a number of equal increments and assuming that the fraction bypassing is of the same order at least in adjacent increments. If a fraction f of the liquor stream leaving increment $i - 1$ bypasses increment i to mix completely in $i + 1$ with the fraction $1 - f$ leaving increment i, a mass balance over increment i is given by

$$u(1-f)C_{i-1} + ufC_{i-2} - uC_i = k \cdot A(C_i - C^x)\delta H \qquad (5)$$

A complete solution for this model with f_i constant is given in the Appendix.

EXPERIMENTAL

It was required to study the effects of crystal size, supersaturation, and liquor velocity on the process. For this purpose batches of different uniform sized crystals were grown for relatively short periods under various conditions of liquor velocity and inlet supersaturation. The discontinuous nature of the experiments necessitated a sensitive and rapid acting temperature control system. Furthermore the system was selected, after some exploration, because its temperature coefficient allowed sufficiently accurate control of C^x and hence the supersaturation without restricting the range of the driving force $C_o - C^x$ too severely. Magnesium sulfate heptahydrate in water was found to suit the requirements.

The crystallizer consisted of a thin walled copper column, A in Figure 1, 4 in. I.D. × 30 in., fitted with narrow vertical windows on opposite sides. A glass counterpart was rejected when it was found to take too long to reach thermal equilibrium during the growth period. The feed/recycle stream was brought in through a calming section fitted to the bottom of the crystallizer. A wire mesh between the calming section and the crystallizer prevented crystals from falling into the former. The spent liquor left the top of the column through a side tube, passed directly to the shell side of the cooler B, was joined by the feed of concentrated solution, and passed back to the bottom of the calming section. A fines separator on top of the crystallizer was removed after some tests as unnecessary.

The cooled spent liquor was recycled from the cooler exit, through a small heater C, controlled from point D further downstream, back to the cooler entry. Heater C served as a final adjustment to the heat balance as explained below. Recycle flow in excess of this first loop passed through a second loop containing temperature controller D and a large capacity heater F. This heater served to simulate the sensible heat of

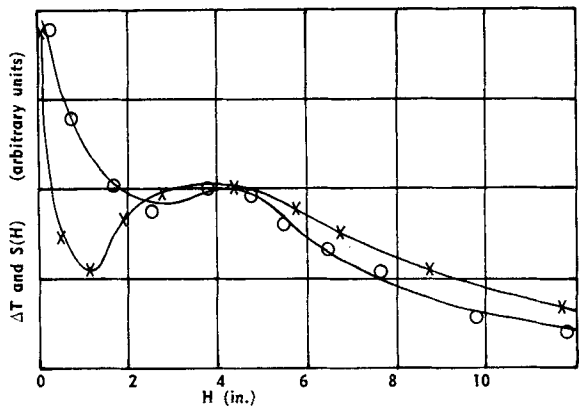

Fig. 2. The attenuation of a thermal signal and the decay of supersaturation in the fluidized bed.

the hot concentrated feed before the latter was started in order to adjust the cooling water flow. Excess liquor flowing in the second loop passed through a rotameter and a density balance G to the calming section. The density balance consisted of a 1-liter flask suspended on a long (8 ft.) spring. Part of the entry liquor stream was diverted through this balance where the density, and hence the concentration, was measured. Excess liquor in the system, equal to the concentrate feed, was drawn off in a constant head device. In earlier experiments the concentrate feed joined the recycle stream before entering the cooler. This arrangement tended to precipitate fine crystals in the cooler, and the effect was eliminated by moving the junction downstream of the cooler.

A weighed bed of selected seed crystals was suspended in a stream of liquor saturated at 20°C. The cooler operated under normal working conditions, the heat extracted being replaced by the feed heat simulator F. The small controlled heater C effected the final adjustment to the heat balance. When the conditions were steady, the concentrate feed was started through a calibrated nozzle into junction E. The feed heat simulator was switched off simultaneously, but heater C remained in operation to maintain the heat balance. The feed stream was continued until the steady state temperature gradient in the bed and column was almost established; the gradient was of the order of 0.016°C./ft. The entry liquor density and the bed height were noted at regular intervals. Samples of liquor were then withdrawn from the crystallizer through the sampling points fixed at various levels up the column. The sampling points were glass tubes, 3/16 in. I.D. inserted through the wall, having their inner ends closed by sintered glass disks. The concentrations of solute in the samples were measured through the density of the solution, determined in a specially constructed balance. Samples were taken over a period of 10 to 15 min. and so represented the average concentrations for that period. A number of methods have been tested for measuring the concentrations in situ. These included temperature scanning with a differential thermometer to yield the integral heat of crystallization as a function of height and a concentration cell method. It was found that the sampling technique was the most reliable. At the end of a growth period the crystals were removed, filtered, washed, dried, and weighed, and their average size was determined. Examinations under a microscope revealed whether any undue amounts of new crystal had formed by spontaneous or secondary nucleation.

RESULTS AND DISCUSSION

It is relevant to the discussion of results and the design of the crystallizer to consider briefly some preliminary exploration. When the temperature scanning method was tested for measuring supersaturation, it was found that a thermal signal from heater C was audible in the crystallizer. The signal had no special wave form, and only its attenuation was measured. The longitudinal attenuation, curve (a) in Figure 2, was similar in shape to the concentration distribution, curve (b). Both curves indicated a large amount of bypassing by the feed/recycle stream at the bottom of the bed, and it was found that the downcomer which served as feed entry caused a vortex ring of rotating suspension at the bottom of the vessel. Since this vortex invalidated the model, it was eliminated. The problem was resolved after some experimenting by introducing the feed/recycle stream through the calming section. With this modification the signal attenuation and the concentration decays were found to be monotonic.

A first estimate of the supersaturation was based on C^x calculated from the average temperature in the crystallizer. The controller developed for this work was capable of switching over less than 0.005°C. range, but owing to other factors the crystallizer temperature was steady only to ± 0.02°C. which corresponds to an uncertainty of 0.011 lb. excess solute/cu.ft. solution in C^x. As a result the lowest supersaturations, c.a. 0.25 lb./cu.ft., were accurate only to ± 4% and the highest, c.a. 0.85 lb./cu.ft., to ± 1.2% on this basis. Concentrations measured by the balance were more accurate, and since the approximate values of C^x showed that the supersaturation decay was first order, C^x was calculated from the values of $C(H)$ for each experiment. Thus when C_1, C_2, and C_3 are the concentrations corresponding to heights H_1, H_2, and H_3 such that $H_2 - H_1 = H_3 - H_2$, it follows that

$$(C_1 - C^x)/(C_2 - C^x) = \exp[m(H_2 - H_1)]$$

and

$$(C_2 - C^x)/(C_3 - C^x) = \exp[m(H_3 - H_2)]$$

whence

$$C^x = (C_1 \cdot C_3 - C_2^2)/(C_1 + C_3 - 2C_2) \qquad (6)$$

Similar solutions can be calculated for the cases of $n < 1$ and $n > 1$, and all the results were tested for these cases. It was found (Figure 3) than $n = 1$ gave consistent results.

The area of crystal surface in unit volume of suspension

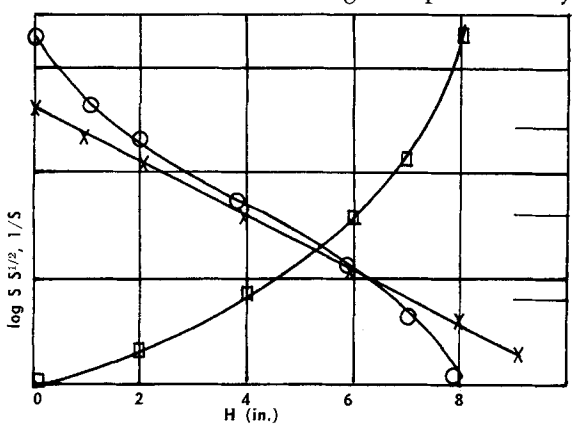

Fig. 3a. Supersaturation vs. height. Tested for n = −½ [○], n = 1 [X], and n = 2 [□] (Experiment 19).

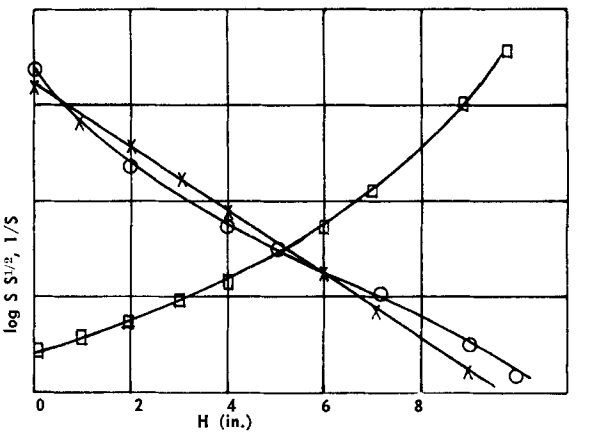

Fig. 3b. Supersaturation vs. height. Tested for n = −½ [○], n = 1 [X], and n = 2 [□] (Experiment 31).

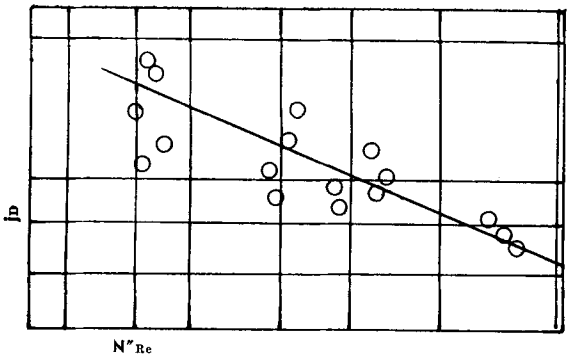

Fig. 4. The correlation of mass transfer rates through mass transfer factor j_D and local Reynolds number N''_{Re}.

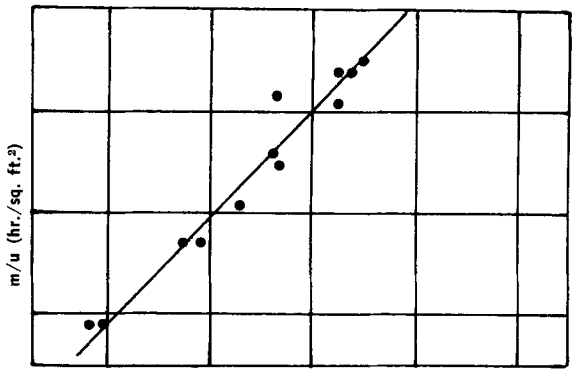

Fig. 5. m/u vs. A/mu.

was calculated as the mean during the sampling period. It was shown that crystals passing a mesh of geometric mean aperture 1 were approximately rectangular prisms of dimensions 1 × 1 × 3.8. The sphere with the same area has a diameter of 2.34 which value was used as a shape factor and to describe the crystal size L. It was also shown that at the low liquor velocities used the bed height was directly proportional to the bed weight. Thus the mean bed height during the sampling period, together with the initial bed height and weight and the initial crystal size, yielded the mean crystal size and surface area. The crystal area in unit volume of suspension follows, since the total volume of suspension is also known. It was considered that arithmetic means were sufficiently accurate because the increase in crystal size during the growth period was $\leq 10\%$.

A number of experiments were rendered invalid for various reasons, but the most frequent cause was a marked change in the fluidization characteristics resulting from partial blocking of the mesh at the bottom of the bed. Blocking at one side produced a pronounced circulation of crystals. The results for two cases of this kind are compared below with satisfactory experiments.

To conform with engineering practice the results of the experiments have been correlated in terms of a j_D factor and the modified Reynolds number $G \cdot L/\mu_l$. A mass transfer coefficient k' may be defined in the same terms through a mass balance over a differential element of suspension to give

$$-G \cdot dS/\epsilon = k'A \cdot S \cdot dH \qquad (7)$$

A selection of typical results is given in Table 1, and Figure 4 shows how they are correlated through the j_D factor and N''_{Re}. The Schmidt number has been retained in the j_D factor to indicate the order of j_D. N_{Sc} was constant throughout all experiments. The equation of the best correlating line was

$$(\epsilon \cdot k'/G)\,(N_{Sc})^{2/3} = 1.3\,(N''_{Re})^{-0.2} \qquad (8)$$

TABLE 1

Mass flow rate, G, lb./(hr.)(sq.ft.) × 10^{-3}	Crystal size, d_L, ft. × 10^3	Bed void fraction	N''_{Re}	Crystal area, A, $ft.^{-1}$	Transfer coeff., k', lb./(hr.)(sq.ft.)	j_D factor, $\frac{k_\epsilon (N_{Sc})^{2/3}}{G}$
3.59	3.56	0.76	0.80	685	10.2	1.26
4.30	6.28	0.72	1.89	406	10.9	1.08
4.30	4.54	0.69	1.42	519	12.1	1.12
5.82	4.46	0.82	1.60	376	20.0	1.65
4.30	2.36	0.80	0.90	526	12.2	1.35
5.20	3.34	0.84	1.04	427	9.6	0.92
5.82	6.10	0.80	2.23	294	14.5	1.17
6.56	8.24	0.70	3.92	332	15.4	0.96

Mass transfer correlations of this general kind are likely to vary considerably with the type of crystallizer and the operating conditions.

Some tests were carried out in order to find the maximum tolerable supersaturation. The cooler had been designed to match the crystallizer but was sufficiently flexible to allow the supersaturation to be increased by progressively lowering the temperature. It was found that a solution, saturated at 20°C. and filtered, could be saturated to the extent of 2.28 lb. excess solute/cu.ft. of solution without causing nucleation. This value decreased to 1.70 lb./cu.ft. with time due, it was thought, to the accumulation of air-borne nuclei. In the presence of a small quantity of seed crystals however a supersaturation in excess of 1.02 lb./cu.ft. gave rise to large amounts of new crystals. The product crystals grown under the highest supersaturation which could be maintained in the presence of seeds, namely 1.06 lb./cu.ft., were of good quality, showing no irregularities of growth as is usually expected (2). The formation of new crystals by an apparently secondary nucleation process has been noted by many workers and would appear to be important in the operation of continuous crystallizers.

The experimental results were also tested by means of Equation (3). It would be expected however that the eddy diffusivity would depend on the modified Reynolds number N'_{Re}. Such a dependence renders Equation (3) intractable, and it was considered reasonable to regard δ_E as constant within an order of magnitude over the range $1 < N'_{Re} < 5$ relevant in the present case. Kramers et al. (7) and Bruinzeel et al. (11) have measured δ_E in fluidized beds in this range, and the former's results would predict $\delta_E \approx 1$ sq.ft./hr. while the latter's would predict $\delta_E \approx 10$ sq.ft./hr. The exponent of Equation (3) was equated with $m \cdot H$ from Equation (4) and rearranged to

$$m/u = 1/\delta_E - (A/mu)\,(k/\delta_E) \qquad (9)$$

The experimental quantities m/u were plotted against A/mu to give a line of slope $-k/\delta_E$ and intercept $1/\delta_E$ (Figure 5). The best line through results selected as being free from criticism yielded

$$\delta_E \approx 29 \text{ sq.ft./hr.}$$

and

$$k = 0.32 \text{ lb./(hr.)(sq.ft.)/cu.ft./lb. } (= \text{ft./hr.})$$

The value of δ_E does no more than establish an order of magnitude, while the value found for k is in reasonable agreement with the value found by Hixson and Knox (12) for the same system. These latter have reported a growth rate constant equal to 0.331 lb.mole/(hr.)(sq.ft.)/mole fraction excess solute at 30.5°C. With their value of 24-300 cal./mole for the activation energy of the process, and converting to the present units, Hixson and Knox's constant becomes

$$k = 0.355 \text{ ft./hr.}$$

This value of k corresponds to the rate expected from molecular diffusion through a stagnant layer at the crystal surface. Thus $k = D_v/x \approx 0.35$ ft./hr. yields $x \approx 5.0 \times 10^{-3}$ ft. with $D_v = 1.81 \times 10^{-3}$ sq.ft./hr. (20°C.).

It may be noted that values of $\delta_E = 76.0$ and 130 sq.ft./hr., respectively, were calculated for two experiments where values for m were low in view of the known values of A and u. It was concluded that a large measure of bypassing had occurred owing to partial blocking of the supporting mesh.

The same experiments were also examined by means of the bypassing model. The bed height was divided into 1- or 2-in. increments, and the mean concentration C_i corresponding to the middle of each increment was read from the graph of $C(H)$. A number of tests were applied to each set of results. An average value for k was calculated for each pair of adjacent increments with the assumptions that no bypassing occurred, that is $f = 0$, and that bypassing occurred. With the assumption that the fraction bypassing in adjacent elements is at least of the same order, values for f were calculated for adjacent pairs. The numerical analysis was simplified by adding

$$u(1-f)C^x + fC^x - C^x = 0$$

to the left-hand side of Equation (5) which rearranges to give

$$(1-f)S_{i-1} + fS_{i-2} - S_i = A \cdot k \cdot \delta H \cdot S_i/u \qquad (10)$$

Abbreviating $A \cdot k \cdot \delta H/u = B$ one writes Equation (10) for adjacent elements as

$$(B+1) = \frac{S_{i-1} + f(S_{i-2} - S_{i-1})}{S_i}$$

and

$$(B+1) = \frac{S_{i-2} + f(S_{i-3} - S_{i-2})}{S_{i-1}} \qquad (11)$$

from which one calculates f and B. The results of such an analysis are shown in Table 2 as the values of B', corresponding to $f = 0$, B, and f for adjacent pairs of increments in a typical acceptable experiment.

From the average values tabulated the growth rate constant is found to be

$$k'(f = 0) = 0.16 \text{ ft./hr.}$$

$$k \text{ [Equation (11)]} = 0.32 \text{ ft./hr.}$$

When the results for all other experiments were analyzed in this way, the growth constant k', calculated on the basis f = 0, was consistently half the value calculated on the basis of a finite amount of bypassing; an average over all the experiments of k [Equation (11)] = 0.30 ± 0.04 ft./hr. was found. The wide scatter in the individual values of f in Table 2 was typical and thought to be due to the severity of the test by comparison with the smoothing inherent in the use of the former model. It may be noted that the experiments quoted above which yielded high values for δ_E gave low values for k when analyzed by the fractional bypassing model.

TABLE 2

Expt. 18; $u = 58.2$ ft./hr. $A = 665$ sq. ft./cu. ft.

H, in.	$S(H)$, lb. excess/cu. ft.	B' ($f = 0$)	B [Equation (11)]	f [Equation (11)]
0	0.455	0.17	0.20	0.13
1	0.387	0.22	0.50	1.20
2	0.315	0.17	0.05	0.53
3	0.270	0.12	0.30	0.70
4	0.240	0.16	0.20	0.26
5	0.207	0.14	0.60	0.80
6	0.180	0.16	0.31	—
7	0.154	—	—	—
8	0.135	—	—	—
9	0.112	—	—	—
10	0.101	avg. 0.16	avg. 0.31	avg. 0.56

Any effects arising from size classification were neglected in the foregoing analyses since seed crystals had been selected to minimize the effects. It is impossible to select exactly identical crystals however, and some experiments, of which the following is typical, were carried out. Samples of crystals were taken from the top and from the bottom of a suspended bed, a distance of 15 in. apart, before and after a growth period. Liquor concentrations were measured as before and the value of exponent m calculated. The average size of a crystal in each of the four samples was measured, the mean area of the seed and product, top and bottom, was calculated, and the corresponding weight increases were also calculated. The mean areas and the weight increments were

Sample	Mean area sq.cm. × 10^2 × ω	Weight increase g. × 10^3
Bottom	1.24 (A_b)	0.683 (ΔW_b)
Top	0.92 (A_t)	0.333 (ΔW_t)

A value $m = -1.46$ was found for the experiment. If exact classification had occurred, the weight increases would have been in the ratio

$$\Delta W_b/\Delta W_t = [A_b \cdot k \cdot S_o \cdot \theta]/[A_t \cdot k \cdot S_o \cdot \theta \exp \cdot (mH)] = 8.4$$

Complete mixing would give all crystals the same average environment, and the ratio of the weight increases would have been the same as the ratio of their areas, namely 1.34. The experimental value ≈ 2.0 corresponds to the growth that would have occurred in an exactly classified bed at points 3 in. apart instead of 15. This result was typical and indicates that the migration of the crystals corresponded nearly but not exactly to complete mixing.

CONCLUSIONS

It was shown that a fluidized bed crystallizer conformed reasonably with the mathematical model proposed. The crystallization of magnesium sulfate obeyed a first-order rate equation for which a growth constant $k = 0.32$ ft./hr. was calculated. This value suggests that the controlling step in the growth was molecular diffusion through a thin stagnant layer at the crystal surface. The concentration decay along the fluidized bed was shown to be due partly to the longitudinal dispersion of the liquor. The extent of the dispersion was calculated as an effective eddy diffusivity of the same order as that found by Bruinzeel (*11*) for a similar fluidized bed. It has been proposed that longitudinal dispersion can be treated as a degree of bypassing of the crystals by the supersaturated liquor, but it appears that measurements of high precision are necessary to test this model.

The effective dispersion would be expected to depend on the crystallizer design, and in the present case it was found to be sensitive to the flow pattern. It has been shown that crystals are not classified even under the best conditions, and the migration of crystals was considered to contribute to longitudinal dispersion.

The operating variables of the pilot scale unit were found to correlate through j_D factors and a modified Reynolds number $G \cdot L/\mu_l$ in a manner expected for mass transfer in a fluidized bed. The operating conditions of the

crystallizer were designed to test a mathematical model however, and the correlation is thought to be specific to the system and conditions under which it was examined.

ACKNOWLEDGMENT

The authors wish to acknowledge helpful discussions in the preparation of this paper with Dr. G. V. Jeffreys (Manchester) and Dr. V. G. Jenson (Birmingham).

NOTATION

A = surface area of crystal per unit volume of suspension, sq.ft./cu.ft.
b = exponent of N'_{Re} in Equation (1).
B = abbreviation for $Ak\cdot\delta H/u$ in Equation (11)
B' = abbreviation for $Ak'\delta H/u (f = 0)$ in Equation (11)
C = concentration of solute, lb./cu.ft. of solution
C_o = concentration of solute in solution entering at bottom of crystallizer, lb./cu.ft.
C^x = equilibrium (saturation) concentration of solute, lb./cu.ft.
dL/dt = average rate of growth of crystal surface normal to itself
D_v = molecular diffusivity of solute in saturated solution, sq.ft./hr.
f = fraction of liquor stream bypassing an element of crystallizer
G = mass flow of liquor based on empty crystallizer, lb./hr. sq.ft.
H = height from bottom of crystallizer, ft.
i = an element of the crystallizer
j_D = mass transfer factor $(k'\epsilon/G)(N_{Sc})^{2/3}$
k = rate constant of crystal growth, ft./hr.
k' = mass transfer coefficient in Equation (8), lb./hr. sq.ft., and also spurious rate constant in Equation (11) with $f = 0$
L = equivalent diameter of a crystal, ft.
m = experimental part of exponent (mH), ft.$^{-1}$
n = exponent of S in rate equation
N'_{Re} = Reynolds number, $L\cdot u\,\rho_l/\mu_l$
N''_{Re} = Reynolds number, $G\cdot L/\mu_l$
N_{Sc} = Schmidt number, $\mu_l/\rho_l\cdot D_v$
S = $C - C^x$, lb./cu.ft.
S_o = $C_o - C^x$, lb./cu.ft.
t = time, hr.
u = liquor velocity, ft./hr.
ΔW = weight increment, g.
x = thickness of stagnant film, ft.

Greek Letters

δ_E = eddy diffusivity, sq.ft./hr.
ϵ = void fraction in fluidized bed
ρ_l = density of liquor, lb./cu.ft.
μ_l = viscosity of liquor, lb./hr. ft.
ω = shape factor in Table 2

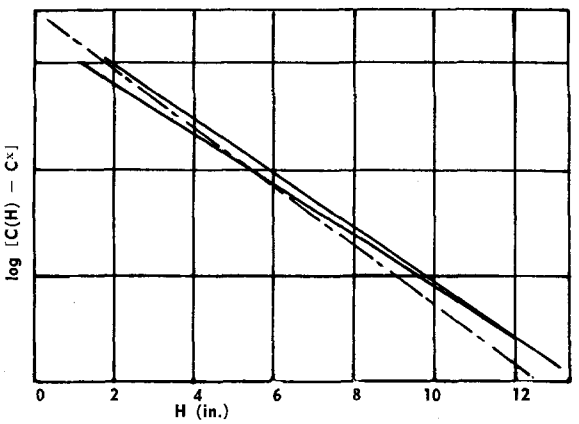

Fig. 6. Log [C(H) — C^x] vs. H for the fractional bypassing model. Upper full line f = 0.10, lower full line f = 0.15, dashed line f = 0.05.

LITERATURE CITED

1. van Hook, A., "Crystallization Theory and Practice," Reinhold, New York (1961).
2. Miller, P., and W. C. Saeman, *Chem. Eng. Progr.*, **43**, 667 (1947).
3. Bransom, S. H., *Brit. Chem. Eng.*, **5**, 838 (1960).
4. Bennett, R. C., *Chem. Eng. Progr.*, **58**, 76 (1962).
5. Bransom, S. H., and A. C. Palmer, *Brit. Chem. Eng.*, to be published.
6. Lemlich, R.. and I. Caldas, *A.I.Ch.E. Journal*, **4**, 376 (1958).
7. Kramers, H., et al., *3rd Congress European Fedn. Chem. Eng., London*, **B.1** (1962).
8. Danckwerts, P. V., *Chem. Eng. Sci.*, **2**, 1 (1953).
9. Wehner, J. F., and R. H. Wilhelm, *ibid.*. **6**, 89 (1956).
10. Levenspiel, O., and K. B. Bischoff, *Ind. Eng. Chem.*, **51**, 1931 (1959); **53**, 313 (1961).
11. Bruinzeel, C., et al., *3rd Congress European Fedn. Chem. Eng. London*, **B.7** (1962).
12. Hixson, A. W., and K. L. Knox, *Ind. Eng. Chem.*, **43**, 2144 (1951).

Manuscript received June 11, 1963; revision received February 17, 1964; paper accepted February 18, 1964.

APPENDIX

The Fraction Bypassing Model

A solution may be obtained for the decay of supersaturation in a fluidized bed by regarding the bed as a number of small stirred tanks in series and allowing part of the stream from each tank to bypass the next in line. For simplicity it is assumed that the suspension density is unform throughout, that the area of crystal in unit volume of suspension is uniform, and that the fraction of stream bypassing each tank as well as the rate constant k are also constant throughout. The bed is divided into a number of elements (tanks) of equal height, and the streams entering and leaving are such that a fraction f of the stream entering element i bypasses element $i + 1$ but mixes completely with the fraction $1 - f$ leaving $i + 1$ upon entering element $i + 2$. A slight complication arises in the bottom element because there is no fraction from a next-but-one lower, but this may be neglected when the number of elements is large. When one abbreviates $A\cdot k\cdot\delta H/u = B$, the mass balances are

$$i = 1; \quad (1-f)C_o - (1-f)C_1 = B(C_1 - C^x)$$

$$C_1 = \frac{(1-f)C_o}{(B+1-f)} + \frac{BC^x}{(B+1-f)}$$

$$i = 2; \quad (1-f)C_1 + fC_o - C_2 = B(C_2 - C^x)$$

$$C_2 = \frac{fC_o}{(B+1)} + \frac{C_o(1-f)^2}{(B+1)(B+1-f)} + \frac{BC^x(1-f)}{(B+1)(B+1-f)} + \frac{BC^x}{(B+1)} \text{ etc.}$$

When one sets $(B + 1 - f) \approx (B + 1)$, the series proceeds to the general term for C_n which is

$$C_n = C_o \sum_{i=1}^{n/2} \frac{(n+1-i)!}{(n+2-2i)!}\,\frac{1}{(i-1)!}\,\frac{f^{i-1}(1-f)^{n+2-2i}}{(B+1)^{n+1-i}} + BC^x \sum_{i=1}^{n/2} \left\{ \frac{(1-f)^{n+1-2i}}{(B+1)^{n+1-i}} \cdot \sum_{r=1}^{i} \frac{(n-i+r)!}{(n-2i)!}\,\frac{1}{(i-r)!}\cdot f^{i-r} \right\} + BC^x \sum_{i=1}^{n/2} \frac{1}{(B+1)^i} \tag{A1}$$

In case n is odd, the upper limit of each summation is $n/2 + 1$. The general term may be rearranged in terms of $(C_n - C^x)$ and $(C_o - C^x)$ when it is evident that the concentration decay follows a course similar to that for the dispersion model and is proportional to exp $(-nB)$, that is to exp $(-A\cdot k\cdot H/u)$. Some numerical results are illustrated in Figure 6. Since the assumption that f_i and A_i are constant must be in some doubt, it is considered that this model needs further exploration.